A Tale of Two Spicy Seas

By Jennifer A. MacKinnon, Jonathan D. Nash, Matthew H. Alford, Andrew J. Lucas, John B. Mickett, Emily L. Shroyer, Amy F. Waterhouse, Amit Tandon, Debasis Sengupta, Amala Mahadevan, M. Ravichandran, Robert Pinkel, Daniel L. Rudnick, Caitlin B. Whalen, Marion S. Alberty, J. Sree Lekha, Elizabeth C. Fine, Dipanjan Chaudhuri, and Gregory L. Wagner

ABOVE: View from the bow of R/V *Sikuliaq*.
Credit Jennifer A. MacKinnon
BACKGROUND: RADARSAT image of the
Beaufort Sea. © *MacDonald, Dettwiler and*
Associates Ltd., All Rights Reserved

> Here, we explore the similarities and differences in these two [spicy] seas by presenting concurrent observations from both using similar tools and techniques. Our hope is to shed light on the more general nature of submesoscale processes and their impacts, and to identify common threads.

ABSTRACT. Upper-ocean turbulent heat fluxes in the Bay of Bengal and the Arctic Ocean drive regional monsoons and sea ice melt, respectively, important issues of societal interest. In both cases, accurate prediction of these heat transports depends on proper representation of the small-scale structure of vertical stratification, which in turn is created by a host of complex submesoscale processes. Though half a world apart and having dramatically different temperatures, there are surprising similarities between the two: both have (1) very fresh surface layers that are largely decoupled from the ocean below by a sharp halocline barrier, (2) evidence of interleaving lateral and vertical gradients that set upper-ocean stratification, and (3) vertical turbulent heat fluxes within the upper ocean that respond sensitively to these structures. However, there are clear differences in each ocean's horizontal scales of variability, suggesting that despite similar background states, the sharpening and evolution of mesoscale gradients at convergence zones plays out quite differently. Here, we conduct a qualitative and statistical comparison of these two seas, with the goal of bringing to light fundamental underlying dynamics that will hopefully improve the accuracy of forecast models in both parts of the world.

INTRODUCTION

The complex and nonlinear dynamics of the near-surface ocean control heat fluxes toward or away from the atmosphere (or, in polar regions, the sea ice). Most regional or global models parameterize these turbulent heat fluxes using one-dimensional mixing schemes (e.g., Large et al., 1994). However, over the last decade, increasing attention has been paid to the role submesoscale processes play in setting upper-ocean stratification and heat fluxes. While "submesoscale" typically refers to a large variety of oceanic motions with spatial scales smaller than a Rossby radius and dynamics that depart from geostrophic balance, here we are specifically interested in the interactions between small-scale lateral and vertical processes, and the ways they conspire to set near-surface heat fluxes, stratification, and the resultant sea surface temperature (Thomas et al., 2008; Shcherbina et al., 2015; Mahadevan, 2016). These processes can induce "restratification": the slumping of lateral gradients into vertical ones, a process that directly competes against the smoothing effects of vertical mixing. When such restratifying processes are significant, traditional one-dimensional mixing schemes will lead to substantial model biases, generally in the direction of over-mixing the upper ocean and producing sea surface temperatures (SSTs) that are "too cold" and mixed layers that are "too deep" (Chowdary et al., 2016, in

this issue). Parameterization of the effects of one such submesoscale instability (a surface-layer-confined baroclinic instability) has produced noticeable improvement in global model biases (Fox-Kemper et al., 2011). However, the full range of submesoscale behavior, principal dynamics, and effects are still poorly understood, in part due to the inherent complexity of many potentially overlapping and superimposed processes, and in part due to a paucity of in situ oceanic observations.

Two synoptic experiments in distant locations provide intriguingly similar views of the nature and consequences of energetic submesoscale fields. The Air-Sea Interactions Regional Initiative (ASIRI) and Ocean Mixing and Monsoon (OMM) program in the Bay of Bengal aimed to better understand and predict near-surface stratification, turbulent heat fluxes, and their effect on SST, with an ultimate goal of improving regional monsoon forecasts (Lucas et al., 2014; Wijesekera et al., in press). The ArctixMix experiment was designed to investigate turbulent mixing and its consequences within the Beaufort gyre, with a goal of better understanding the processes contributing to seasonal and longer-term storage, transport, and vertical mixing of heat, both in exchange with the atmosphere and in the melting of sea ice.

Though different in latitude and temperature, the Arctic Ocean and the Bay

of Bengal (BoB) have some surprisingly similar features, represented schematically in Figure 1. Both share the globally unusual feature that stratification, within and at the base of the surface layer, is largely set by salinity controlled by large quantities of freshwater from river runoff in both places, monsoonal rains in the BoB, and ice melt in the Arctic that lead to O(1 psu) salinity changes, sometimes on very small (kilometers or less) scales. Temperature is often comparatively passive in its contribution to density in both seas, particularly in the Arctic where the thermal expansion rate is extremely small (Timmermans and Jayne, 2016). We use the term "spicy seas" here in a somewhat colloquial sense to represent oceans in which there is significant temperature-salinity (T-S) variability along an isopycnal. Subsurface temperature maxima are commonly observed in both locations, created in part by advection of river waters or ice melt over locally warmed surface mixed layers. These surface layers, when mixed via turbulence, lead to divergent heat fluxes (upward toward the surface and downward at depth), and may be important players in upper-ocean heat budgets (Timmermans, 2015; and Thangaprakash et al., Mahadevan et al., Lucas et al., Shroyer et al., Johnston et al., Jinadasa et al., and Warner et al., 2016, all in this issue). Finally, both seas

display rich lateral structure in near-surface salinity, as freshwater input is stirred by active mesoscale eddy fields (Sengupta et al., 2016). Where water masses collide in that stirring process, fronts are created. Three-dimensional circulation at those fronts often leads to subduction and interleaving of water masses above and below each other, creating complex patterns of vertical stratification and making any purely one-dimensional view of turbulent heat fluxes as a vertical process inappropriate (Timmermans et al., 2012). Here, we explore the similarities and differences in these two seas by presenting concurrent observations from both using similar tools and techniques. Our hope is to shed light on the more general nature of submesoscale processes and their impacts, and to identify common threads.

INSTRUMENT AND EXPERIMENTAL DESIGN

Simultaneous, month-long process experiments were conducted in the Arctic and the Bay of Bengal during late summer 2015 (Figure 2). On R/V *Sikuliaq*, 18 scientists from the United States, France, Norway, and Australia performed process experiments to study the effects of turbulent mixing and lateral advection on heat fluxes in the Arctic Ocean. Observations from the Arctic were recorded from

August 24–September 26, 2015, and sampling was conducted within the Beaufort and Chukchi Seas, including in areas with dense pockets of multiyear ice. In the BoB, 23 researchers from the United States and India aboard R/V *Revelle* (August 23 to September 21, 2015) performed coordinated experiments with the Indian ORV *Sagar Nidhi*, which also hosted both Indian and US scientists.

All three ships (R/Vs *Sikuliaq* and *Revelle* and ORV *Sagar Nidhi*) were equipped with similar sets of instruments tuned to measure upper-ocean submesoscale density, velocity, and turbulence (Figure 3). The main instruments used on R/V *Sikuliaq* included a towed body; the Shallow Water Integrated Mapping System (SWIMS) measuring conductivity, temperature, depth (CTD), and horizontal currents; and the Modular Microstructure Profiler (MMP) for turbulence (both developed by M. Gregg, University of Washington). Similarly, ORV *Sagar Nidhi* utilized an underway CTD and a Rockland Scientific vertical microstructure profiler (VMP) for turbulence profiling. R/V *Revelle* used a Fast CTD (developed by R. Pinkel, Scripps Institution of Oceanography) for underway T-S profiling (Lucas et al., 2016, in this issue) and a Rockland VMP for turbulence profiling (Jindasa et al., 2016, in this issue). All three ships also sampled near-surface salinity and temperature from their flow-through systems.

Additionally, both US vessels (R/Vs *Revelle* and *Sikuliaq*) towed bow-mounted chains with fast-response thermistors and CTDs distributed over the upper 10 m to 20 m. *Revelle* also deployed ROSS—a remotely operated kayak that performed parallel tracks to *Revelle* and *Nidhi*, sampling density in the upper 15 m and velocity in the upper 60 m (Box 1). Limited bow-chain measurements were also taken from an ad hoc system rigged on the *Sikuliaq* workboat. Pressure measurements were used to remove the effect of surface wave heaving from bow-chain data. Cruise paths for 2015 field seasons for R/Vs *Sikuliaq* and
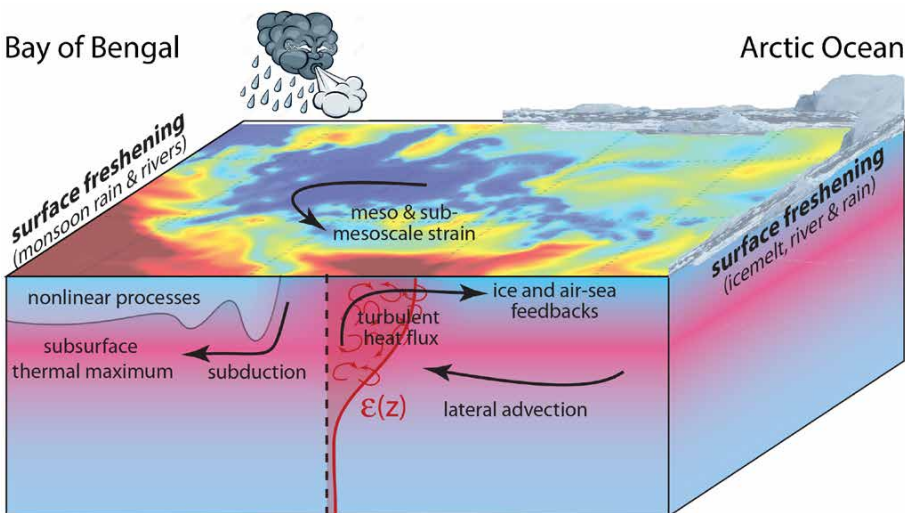

FIGURE 1. Cartoon of various upper-ocean processes at work in both the Arctic Ocean and the Bay of Bengal.

Revelle and ORV *Sagar Nidhi* are shown in Figure 2, colored by near-surface temperature from each ship's flow-through CTD system. All three ships were equipped with multiple acoustic Doppler current profilers for measuring velocity in the upper few hundred meters.

NEAR-SURFACE STRUCTURE

Both seas have thin but stratified surface layers where salinity generally determines density. Figure 4 shows long underway CTD sections from both experiments. In both cases, there is a relatively fresh 10–30 m surface layer that is separated by the temperature-stratified ocean below by an extremely sharp (3–4 psu) halocline. Within the surface layer, complex lateral structure is present in both temperature and salinity, with gradients at a wide range of scales (top panels in Figures 4 and 5). Visible
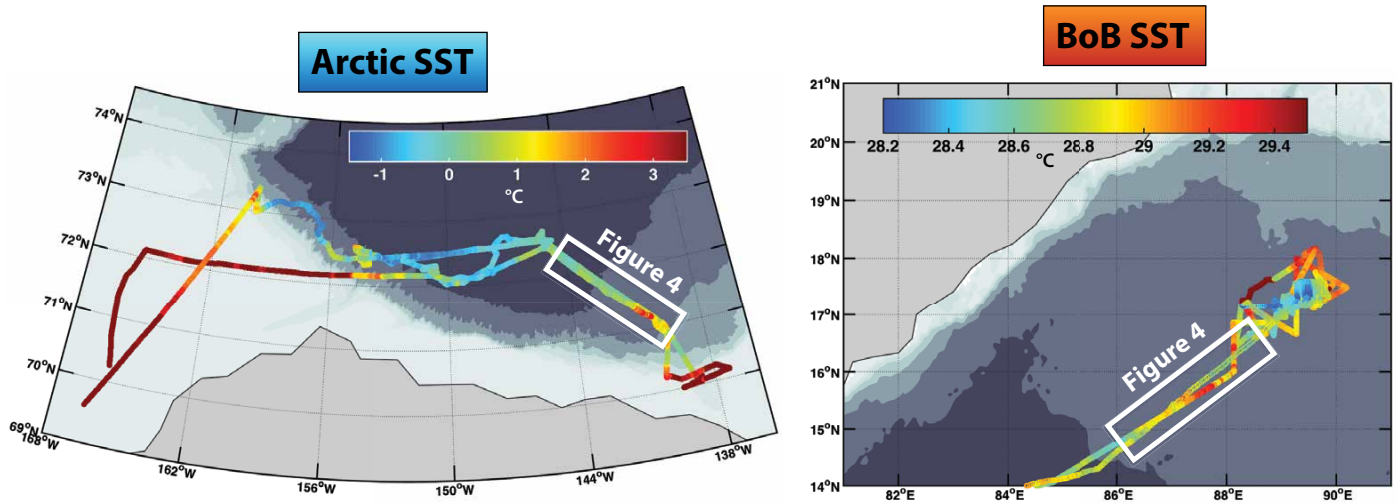

FIGURE 2. Sea surface temperature (SST) as observed from three ships in the Arctic Ocean and in the Bay of Bengal (BoB) during August–September 2015.
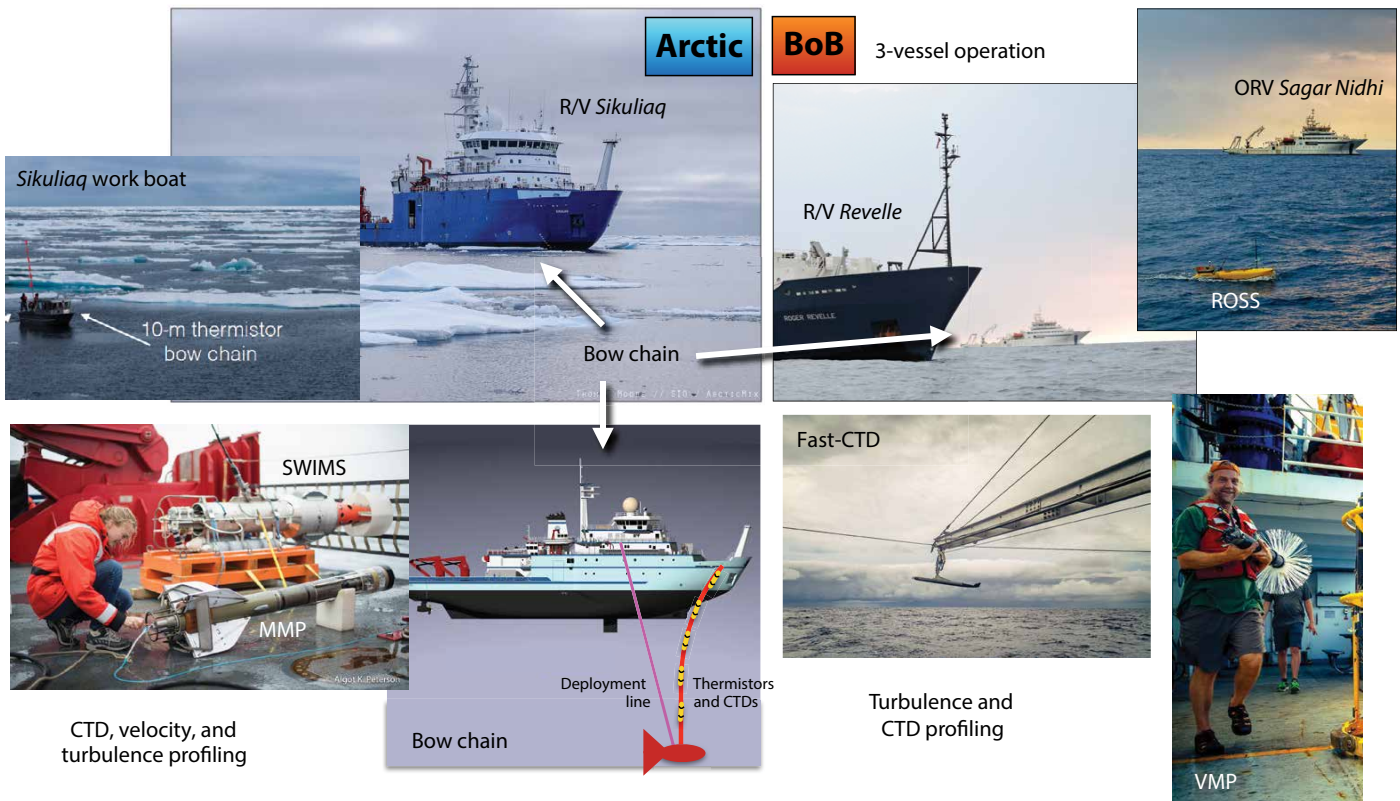

FIGURE 3. A selection of instruments and vessels used in the Arctic Ocean and the BoB in late summer 2015.

Box 1. The Robotic Oceanographic Surface Sampler

**By Jonathan D. Nash, June Marion, Nick McComb, and Andy Pickering**

The Robotic Oceanographic Surface Sampler (ROSS; http://makani.coas.oregonstate.edu/ross/Overview.html) is a semi-autonomous gas-powered kayak developed at Oregon State University to investigate the fine-scale dynamics of the upper ocean. Equipped with a 300 kHz acoustic Doppler current profiler and towed thermistor/CTD chain, ROSS can rapidly carry out 100–200 km long missions to sample the complex three-dimensional flow that characterizes the submesoscale. While originally intended to navigate waters too dangerous for manned vessels (e.g., near the termini of calving glaciers), it also has the unique capability of being able to obtain uncontaminated data about the upper ocean from a surface-following perspective, making it useful for air-sea interaction studies.

In its maiden open-ocean deployment in the Bay of Bengal in September 2015, ROSS was deployed in a coordinated sampling effort with two research vessels (R/V *Revelle* and ORV *Sagar Nidhi*). The use of three "ships" allowed simultaneous parallel transects to be occupied, permitting instantaneous gradients of density and velocity to be computed at multiple separations (1, 2, and 3 km;

Figure B1d). In addition to providing lateral context, ROSS also provides a very detailed perspective of the ocean's upper few meters (Figure B1c), a region that is challenging to sample from a larger research vessel. Freshwater layers that are 5–10 m thick are common in the Bay of Bengal, and are found to have sharp horizontal gradients in which temperature and salinity change by 0.2°C and 0.2 psu over only 5 m laterally; horizontal gradients spanning a broad spectrum of horizontal scales are ubiquitous in the bay. Undulations in these thin layers are also evident and suggestive of a dynamic instability, driven either by wind, waves, or internal shear. In addition, convective instabilities also become visible when data are examined over very small temperature ranges; 10 m deep plumes carrying 0.01°C colder waters are a means of mixed layer deepening at night. We anticipate ROSS and similar semi-autonomous surface craft becoming important components of high-resolution upper-ocean and air-sea exchange processes studies in the future.

AUTHORS: Jonathan D. Nash, **June Marion**, **Nick McComb**, and **Andy Pickering** are all at the College of Earth, Ocean, and Atmospheric Sciences, Oregon State University, Corvallis, OR, USA.

FIGURE B1. (a) The Robotic Oceanographic Surface Sampler (ROSS) being deployed from the fantail of R/V *Revelle*. (b) ROSS heading off on a mission; ORV *Sagar Nidhi* in the background. *Photo credits: San Nguyen* (c) Sections of temperature obtained by ROSS reveal particularly sharp fronts, horizontal undulations, and convective instability associated with nighttime sea surface cooling. (d) Three simultaneous velocity transects permit vorticity to be computed at multiple different scales.
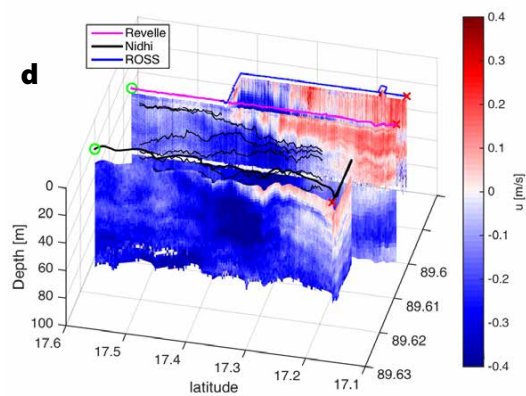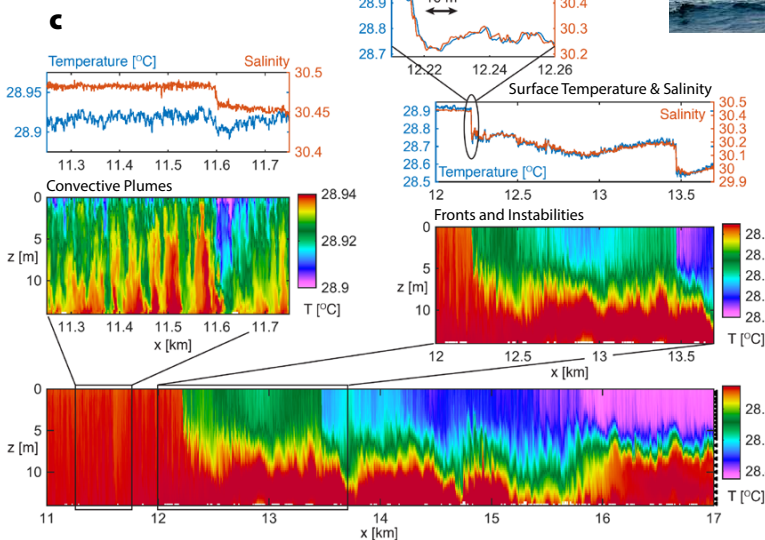
structures reflect crossing of meso-scale eddies (e.g., the freshest near-surface salinities in the lower right panel of Figure 4) and spreading of regional freshwater inputs (e.g., presence of comparatively warm, fresh Mackenzie River water near the beginning of the Arctic section). Temperature is nearly a passive tracer in both cases, contributing to approximately 10% of the lateral density variance, as indicated within Figure 4. Both seas frequently show subsurface temperature maxima, whose implications for turbulent heat fluxes will be discussed below.

Spectral analysis is frequently used in oceanography, and fluid dynamics in general, to study problems in which certain sorts of dynamical processes produce motions that are self-similar across a range of scales. Such motions often produce spectral amplitudes that vary according to the frequency or wavenumber raised to some power, creating a straight line on log-log plots. This type of "power law" behavior has been explored in oceanographic data by numerous investigators, including Ferrari and Rudnick (2000), Callies and Ferrari (2013), Klymak et al. (2015), and Kunze et al. (2015). Horizontal spectra of temperature from the various shipboard systems indicate more formally the contributions of different scales of

lateral variability to temperature variance (Figure 5). Temperature variance in the surface layer is plotted as a function of horizontal wavenumber (Figure 5a). In the lowest wavenumber range (largest horizontal scales), there are markedly different slopes between near-surface temperature spectra from the BoB (warm colors) and the Arctic (cool colors). The Arctic data have a –3 spectral slope, which is theoretically associated with potential energy of quasi-geostrophic motions and has been observed previously in the Arctic (Charney, 1971; Timmermans et al., 2012; Timmermans and Winsor, 2013; Marcinko et al., 2015). In contrast, the BoB data in this example
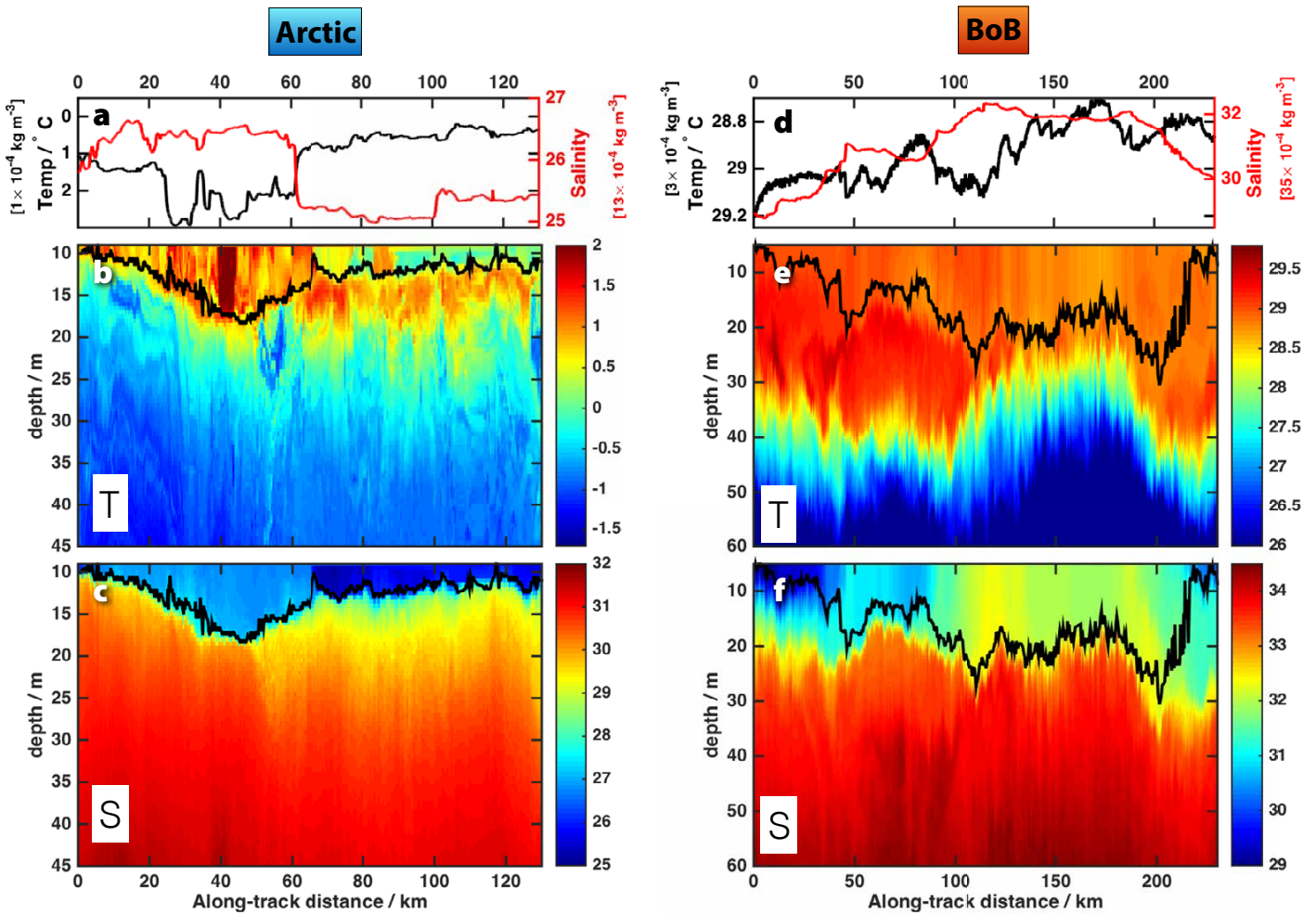

FIGURE 4. Observations of upper-ocean temperature and salinity from the Arctic (left) and the Bay of Bengal (right). (a) and (d) Near-surface temperature (black) and salinity (red) from ships' flow-through systems along the transects indicated with the magenta boxes in Figure 2 (left) from the Arctic and (right) from the BoB. Text to the left and right of the axis labels in (a) and (d) indicate the variance level these temperature and salinity changes contribute to density. (b) and (e) Subsurface temperature from the SWIMS towed body (Arctic) and the Fast CTD (BoB) along the associated transect lines. (c) and (f) Subsurface salinity from SWIMS (Arctic) and Fast CTD (BoB). In the middle and lower rows, the black contours indicate the vertical extent of the surface layer, defined here as the depth at which density is within 0.5 kg m^{-3} of its lowest value.

exhibit a –2 spectral slope; the same slope persists in almost all long BoB sections acquired during this experiment (not shown). This –2 slope is characteristic of an ocean dominated by fronts; sharp discontinuities or abrupt jumps in temperature project equal temperature gradient variance onto all scales, at least all scales larger than the width of the front, leading to temperature spectra with a –2 slope (Ferrari and Rudnick, 2000). The BoB is known to be extremely rich in fronts (Sengupta et al., 2016). Temperature spectra at low wavenumbers have been observed with a –2 slope in a range of other experiments, such as the North Pacific Spice experiment (green, Figure 5c; Ferrari and Rudnick, 2000; Cole et al., 2010) and in recent observations in the Atlantic (Kunze et al., 2015).

Moving to smaller scales (higher wavenumber; 2×10^{-3} to 2×10^{-2} cpm),

observations from both seas surprisingly collapse onto a remarkably similar –1 slope. Other sections from both experiments (not shown) also frequently display –1 slopes within this wavenumber range, with some variability in spectra level. At times, the wavenumber range of this portion is narrow enough that it cannot be distinguished from the sum or overlap of steeper (shallower) spectra at lower (higher) wavenumbers, but for other examples, such as that shown in Figure 5, there appears to be a –1 power law behavior over roughly a decade of wavenumbers. The interpretation for this is not entirely clear. One common interpretation is that the tracer (temperature) is experiencing nonlocal stirring, whereby the fluid is being stirred by motions that have characteristic scales either larger or smaller than the scales over which tracer variance may develop through filamenting and stirring.

Here, the –1 slope is at horizontal scales of about 500 m down to 50 m. At these scales, three-dimensional turbulence is not a reasonable interpretation. Instead, one possibility is that this range of wavenumbers is a "submesoscale Batchelor regime," in which energetic submesoscale instabilities at slightly larger scales stir and filament temperature (Batchelor, 1959; Smith and Ferrari, 2009). The responsible stirring rods are then posited to be just a bit larger scale than the low-wavenumber end of this regime, on the order of one or several kilometers. Some types of submesoscale instabilities, such as mixed layer instability (MLI; Boccaletti et al., 2007), a type of baroclinic instability confined to the surface layer, are thought to have dominant lateral scales on the order of the surface-layer Rossby radius (Callies et al., 2016). This scale (NH/f, where N is the buoyancy frequency within the
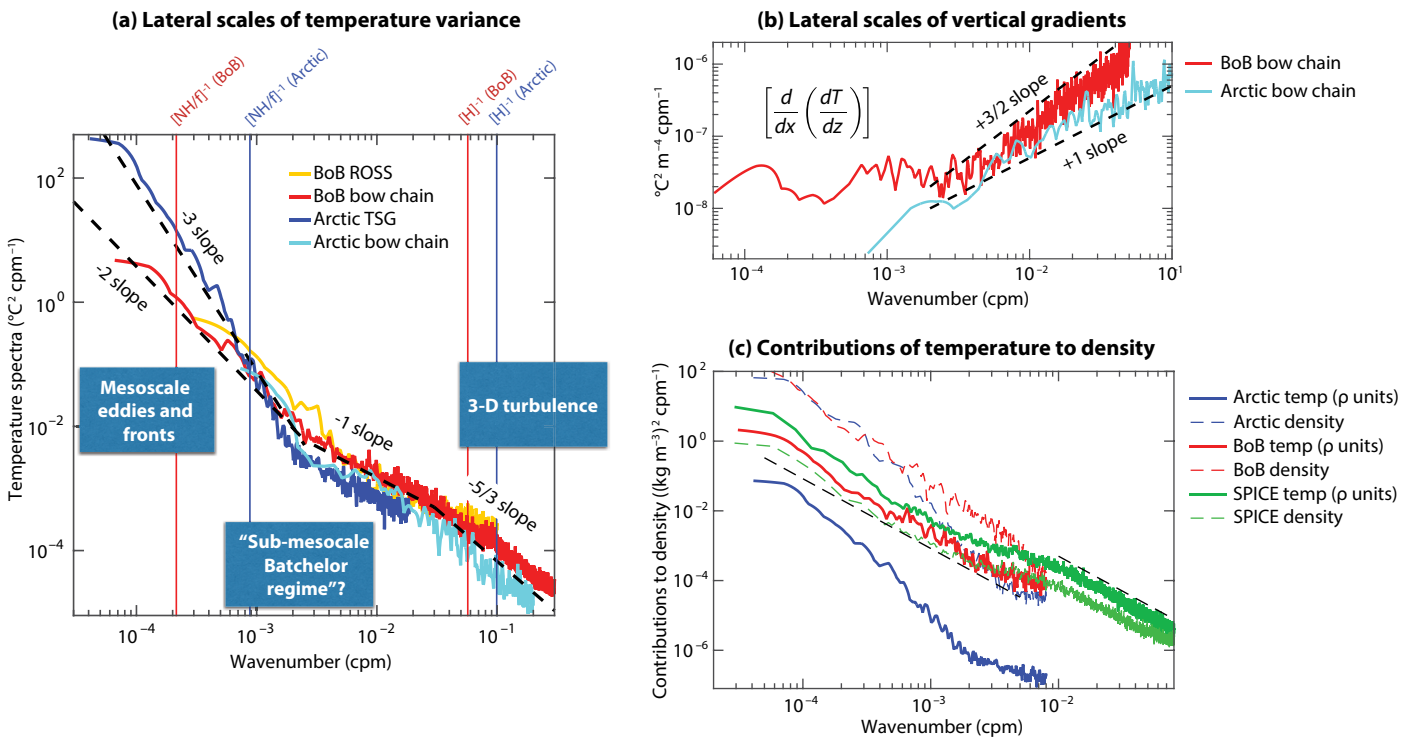

FIGURE 5. Lateral spectra of near-surface temperature measured from sections in the Arctic Ocean and the Bay of Bengal. (a) Lateral scales of temperature variance spectra from the Bay of Bengal R/V *Revelle* bow-chain data (red), from ROSS bow-chain data (orange), from ORV *Sagar Nidhi* flow-through data (magenta), from Arctic shipboard flow-through data (blue), and from Arctic bow-chain data (cyan). Spectra have not been scaled or shifted in any way. Several suggestive power law slopes are indicated and labeled. The four vertical lines are the scales of surface layer Rossby wavenumbers (NH/f) for these sections (left two lines) and the inverse of the surface layer depth (right two lines), as potentially relevant indicators of changing dynamics. (b) Lateral scales of vertical gradients of temperature from the BoB bow chain (red, differenced between 8.5 m and 2.5 m depth) and Arctic bow chain (blue, differenced between 3 m and 13 m depth). (c) Assessment of the contributions of temperature to density spectra from the BoB bow chain (red) and Arctic bow chain (blue). Observations from the 1997 Spice Experiment SeaSoar profiles (Ferrari and Rudnick, 2000) are included for comparison (green). Density spectra are plotted with thick solid lines and temperature spectra with thin dashed lines.

surface layer and H is the surface layer depth where the surface layer is calculated as the depth range in which density does not exceed 0.5 kg m^{-3} above its shallowest value) is indicated with red and blue vertical lines for both seas. Alternately, the spectral slope could be created by stirring by energetic stirring rods with ~50 m or smaller scales; such motions could be any number of three-dimensional turbulent phenomena, such as Langmuir cells (Smith et al., 2015). Internal waves may also contribute to variance in these wavenumber ranges (Callies and Ferrari, 2013; Klymak et al., 2015), though they typically present with steeper slopes. Ongoing analysis will consider the possibility of evanescent internal wave motions within the surface layer in interpreting these observations.

At yet smaller scales (wavenumber above ~3 × 10^{-2} cpm or horizontal scales smaller than ~30 m), the BoB data show a transition from a –1 to a –5/3 slope. This is the point at which the horizontal scale is of the same order as the surface layer depth, and three-dimensional turbulence driven by Langmuir cells or other types of convective mixing are likely present (e.g., Belcher et al., 2012; Smith et al., 2015). The Arctic lateral temperature spectra show similar transitions to steeper slopes at higher wavenumbers.

Box 2. Another Comparison on the Other Side of the Arctic

By R. Venkatesan, K.P. Krishnan, and Divya David

On the other side of the Arctic lies Kongsfjorden, a northwest-southeast-oriented fjord located in the West Spitsbergen area of the Svalbard Archipelago. As with the ArcticMix data, measurements from this part of the Arctic show striking similarities to that of the BoB, especially during summer (Varkey et al., 1996; Schott and McCreary, 2001; Svendsen et al., 2002; Cottier et al., 2005). Similarities include overall physical setting, seasonality, freshwater discharge (glacier melt in Kongsfjorden and river runoff in the BoB), temperature inversions, strong salinity-dominated upper-layer stratification (Subramanian, 1993; Prasad, 1997; Svendsen et al., 2002), horizontal density fronts and vertical density variations (Cottier et al., 2005), eddy activity, tidal influences, and high sedimentation rates, as well as the role entrainment plays in water mass formation in these regions. Hydrography measurements were obtained using a portable CTD in August 2015 along the main axis of Kongsfjorden (Figure B2, left panels). The time series from moored measurements at central Kongsfjorden (Figure B2, right panels) show sharp lateral as well as vertical temperature-salinity gradients that resemble the BoB observations. The daily time series of temperature and salinity measured in central Kongsfjorden and the BoB using India's IndARC multisensor mooring and the Research Moored Array for African-Asian-Australian Monsoon Analysis and Prediction (RAMA), respectively, during the peak summer months of August and September 2014 showed how rapidly the temperature and salinity varied temporally, an indication of variation in the strength of the lateral fronts in the fjord. The features observed between the areas were strikingly similar. Thus, Kongsfjorden can act as a miniature laboratory to understand Bay of Bengal processes in detail due to its size (21 km in length and 5–10 km in width) and easy field accessibility in addition to the many similarities of these two regions. With the growing number of high-latitude measurements underway, we hope that further comparisons between BoB and a variety of Arctic data sets will continue to provide generalized dynamical insights that will lead to development of new, physics-based parameterizations and help improve both monsoon and Arctic ice melt forecasts.

AUTHORS: **R. Venkatesan** is at the National Institute of Ocean Technology, Chennai, India. **K.P. Krishnan** and **Divya David** are at the National Centre for Antarctic and Ocean Research, Goa, India.
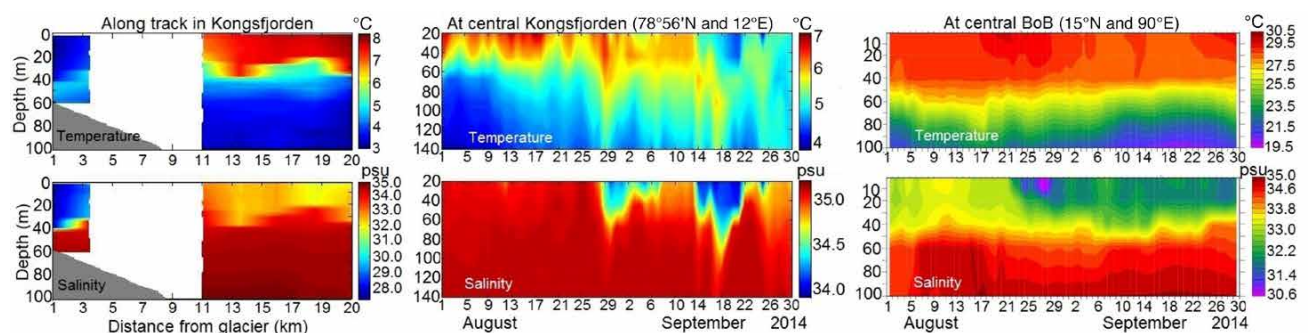

FIGURE B2. (left panels) Vertical water column temperature (upper panel) and salinity (lower panel) along track in Kongsfjorden from CTD measurements in August 2015. Gray color shows bathymetry. (middle and right panels) Daily time series measurements of temperature-salinity from central Kongsfjorden and the BoB during August–September 2014 from IndARC and Research Moored Array for African-Asian-Australian Monsoon Analysis and Prediction (RAMA) moorings, respectively.

It is noteworthy that spectral amplitudes in the –1 and –5/3 regimes show remarkably similar amplitudes between Arctic and BoB data, differing by a factor of three or less in these dramatically different environments.

Though spectra from the Pacific Spice experiment (Ferrari and Rudnick, 2000) show similar –2 spectral slopes at low wavenumbers (thick green line, Figure 5c), these spectra differ substantially from the Arctic and BoB data in the relationship between temperature and density. Ferrari and Rudnick (2000) show that in the Pacific, as in many oceans (Rudnick and Martin, 2002), near-surface temperature and salinity are compensated (similar in magnitude but opposite in sign in their contributions to density) at a wide range of scales. One method of making this assessment is by comparing a horizontal spectrum of density (dashed green line, Figure 5c) versus the spectrum that represents temperature's contribution to density (solid

green line, Figure 5c). The latter is always larger than the former for the Spice data, which is only possible if there is substantial compensation at all scales. In the BoB the opposite is true, with a density spectrum (dashed red line) an order of magnitude larger than temperature contributions to density (solid red line) at all scales, possibly converging at the highest wavenumbers. This is consistent with the observations in Figure 4 that temperature has a 10% contribution to density. In the Arctic, the situation is yet more

dramatic, with several orders of magnitude difference between a typical density spectrum (dashed blue line) and temperature's contribution to density (solid blue line); at this point in the equation of state, the thermal expansion coefficient is extremely small—on average only 1/30th of the value in the Bay of Bengal. Note that the Arctic spectra shown here are typical of mid-Beaufort gyre measurements, whereas the data in Figure 4 include warmer Mackenzie River water where temperature has a slightly larger contribution to density.

CONSEQUENCES FOR TURBULENT HEAT FLUXES

The strength, scales, and character of submesoscale motions in both the Arctic Ocean and the BoB influence a wide range of processes. Some types of submesoscale instabilities (e.g., Fox-Kemper et al., 2011) are associated with restratification, where the potential energy housed in lateral gradients is released to the growing kinetic

energy of the instability; once the instability has run its course and dissipated (through even smaller-scale, unidentified processes), the next result is that the lateral gradients have "slumped" into vertical stratification. Lucas et al. (2016, in this issue) and Sarkar et al. (2016, in this issue) discuss in detail these restratification and subduction processes and comment on their importance. Here, we show that the resultant small lateral-scale variability in stratification has important consequences for turbulence mixing.

The existence of lateral variability in vertical gradients can be quantified in a statistical sense by looking at characteristic horizontal scales of vertical gradients within the surface layer. Figure 5b shows the horizontal variability of vertical temperature gradients, which is not commonly plotted, yet illustrative. In the BoB, the temperature spectrum is flat at lower wavenumbers (red, Figure 5b), indicating that there are equal contributions to stratification changes at a range of different lateral scales; this is again consistent with the dominance of fronts. However, at smaller scales (wavenumbers greater than 1×10^{-2} cpm), the red line takes on a positive slope. For wavelengths smaller than about a kilometer, lateral gradients in vertical stratification become increasingly important. The Arctic observations from the bow-chain data (cyan, Figure 5b) show similar behavior for scales smaller than ~1 km.

Next, we argue that this small-scale lateral variability in stratification produces dramatic and nonlinear responses in turbulent vertical mixing and associated vertical heat fluxes. To illustrate this process, Figure 6 shows example sections of microstructure measurements from both seas. In both cases, a subsurface temperature maximum is visible, and density stratification in the upper ocean has a complex, layered structure (Figure 6a,c). T-S plots in each experiment (Figure 6b,c) show significant interleaving, with some of the T-S variability between profiles mirrored in depth variability in each profile; this interleaving points to complex stirring and subduction processes relevant in setting the horizontally patchy vertical stratification. The bottom panels in Figure 6 (a and d) demonstrate how the turbulent dissipation rate (ε) responds sensitively to the detailed structure of stratification, as is often the case (Jinadasa et al., 2016, in this issue). For example, the band of elevated dissipation between 15 m and 20 m depth in the BoB (third panel in Figure 6d) is coincident with the band of high stratification in this depth range, consistent with turbulence driven

by shear instability, as shear also generally hugs vertical density gradients. In the Arctic (Figure 6a), the turbulent dissipation rate is elevated into the vertically migrating high stratification layer at 10–20 m depth. Ongoing work (not shown here) attempts to interpret these patterns using velocity shear data and Richardson number calculations.

A SPICY WORLD: CONCLUSIONS AND CONFUSIONS

Though the two seas considered here are half a world apart and not an obvious pairing, there are some surprisingly interesting and thought-provoking similarities and differences between them. Though their temperature differences are as extreme as it gets in the ocean, their temperature spectra at medium and small length scales line up strikingly well with each other at moderate to small scales (Figure 5). As described above, this alignment suggests similarities in the fundamental physics governing the behavior in both submesoscale and turbulent processes. Ongoing analysis will consider the implications of both these features for dissipation rates of thermal variance in both locations.

In contrast, the large-scale temperature gradients are quite different in the two seas, both in absolute values and in spectral power-law shapes, suggesting different dynamics. The BoB large-scale spectra are consistent with lateral temperature changes largely being in the form of multiple discrete fronts—as is frequently found in other oceans. The Arctic spectra at low wavenumbers are steeper and not consistent with temperature fronts as a dominant feature. Instead, the spectra show large temperature gradients associated with the largest-scale circulation patterns in the basin. Why fronts

Small-scale lateral gradients in sub-surface temperature and turbulence
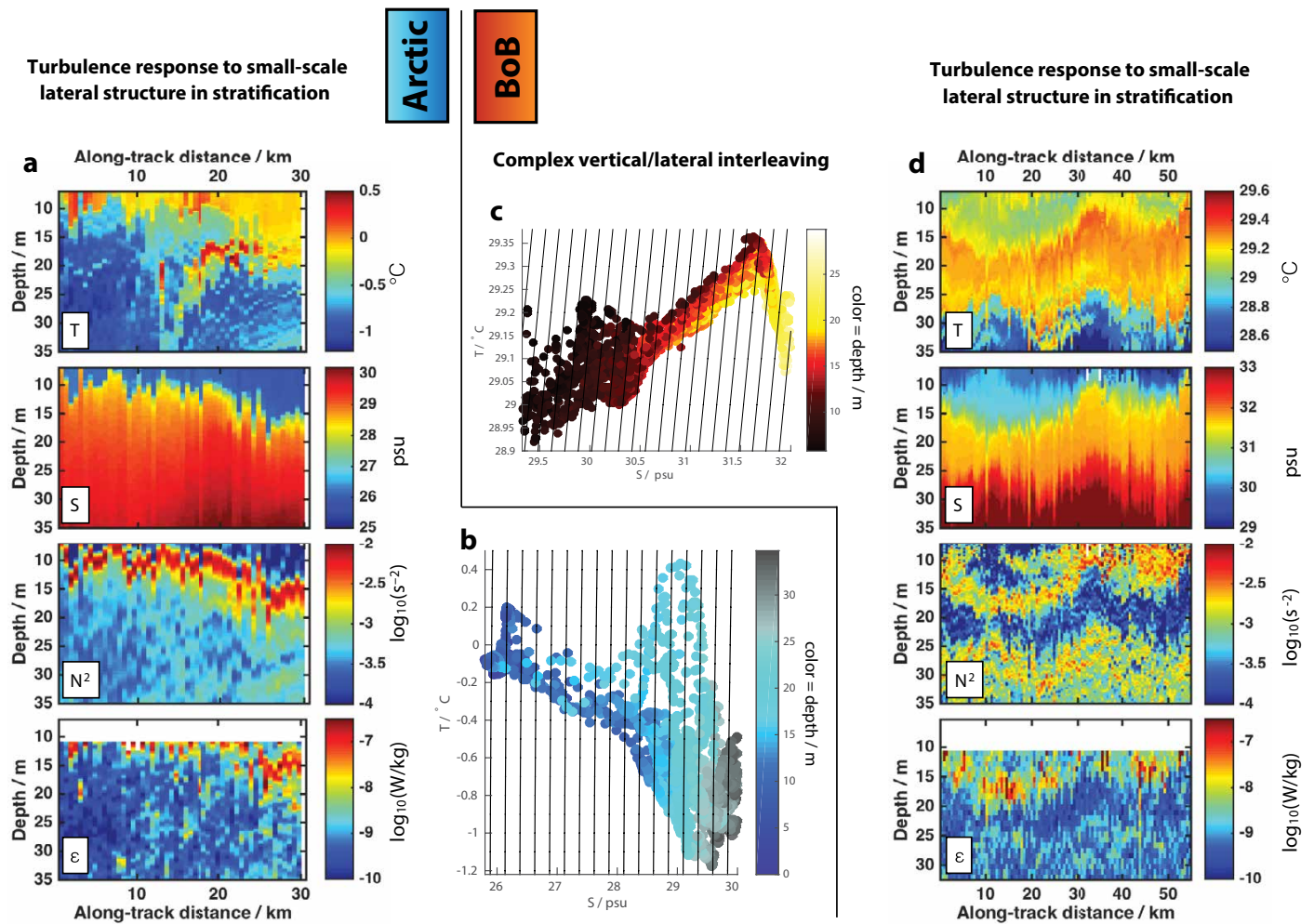

FIGURE 6. Examples of turbulent mixing and observed heat flux from the Arctic Ocean (left) and the Bay of Bengal (right). (a) Modular Microstructure Profiler (MMP) turbulent microstructure observations near 143°W, 72°N on September 2, 2015; panels from top to bottom are temperature, salinity, stratification as indicated by the buoyancy frequency (N^2), and the turbulent dissipation rate (ε), data for which is blanked out in the upper 12 m due to potential ship wake contamination. (b) T-S data for this period, with points color coded by depth. (c) T-S data taken near 89°E, 18°N on September 13, 2015, same panels as in (a). (d) Vertical microstructure profiler (VMP) turbulent microstructure observations from this time period.

would not be as prevalent in the colder, higher latitude spicy sea is an open question. Timmermans et al. (2012) notice the –3 slope in Ice-Tethered Profiler data from the Arctic and speculate that the difference between that slope and the –2 slope commonly observed in lower latitudes is related to ice cover. Marcinko et al. (2015) compare these data with a wider variety of Arctic measurements, and find a –3 slope regardless of ice cover, and instead suggest that the Arctic behavior is dynamically related to strong upper-ocean salinity stratification, which in turn is related to ice but persists even in ice-free conditions. Our observations complicate that interpretation, as salinity stratification in both oceans as profiled here is very similar, both qualitatively and in the magnitude of the N^2 values shown in Figure 6, yet there are distinctly different low wavenumber spectral slopes. It seems as though something in the Arctic environment is suppressing the frequent frontogenesis process that leads to a –2 slope in the BoB. There are a few other observations of –3 spectral slopes at low horizontal wavenumbers (e.g., Samelson and Paulson, 1988; Wang et al., 2010; Rocha et al., 2016), but the relevant feature unifying these examples is unclear.

Improved forecast models require accurate parameterizations of upper-ocean turbulent heat fluxes in order to accurately predict SST. With a few exceptions, most large-scale models employ one-dimensional vertical mixing schemes. In some parts of the world, that may be appropriate, but evidence indicates such schemes systematically fail in environments like the BoB (Wijesekera et al., in press). There are many potential reasons for that failure, including a variety of types of missing physics, but one process that all one-dimensional mixing models are sensitive to is vertical stratification. Stratification sets the Richardson number, upon which the parameterized strength of turbulence depends, which sets the entrainment rate, and sets the relationship between prescribed turbulent mixing and heat fluxes.

Here, we show that in both the Arctic Ocean and the BoB there are significant variations in near-surface properties (temperature, density, and vertical stratification) at small lateral scales. As stratification changes over lateral scales of kilometers and less, the strength of turbulent mixing changes by orders of magnitude. Models that do not accurately represent such stratification will not accurately predict the net effect of turbulent mixing. Development and refinement of parameterizations that can represent such features depends on improved understanding of the underlying physics. The existence of portions of spectral space with defined power law behavior (quasi-straight lines in Figure 5) points to differing physical processes dominating at different scales. At lateral scales on the order of the surface layer depth and smaller, three-dimensional turbulence appears to often be at play; work is underway in both basins to better understand how the strength of this type of turbulence varies with wind and wave forcing, surface buoyancy input, stratification, and other nonlinear processes. At larger scales (hundreds of meters to kilometers), a transition in underlying dynamics indicates different processes at work; stirring by energetic motions of order NH/f (the surface layer Rossby radius) is one possible explanation in need of further exploration. The variety of other frontal instability processes described in this issue of *Oceanography* may also contribute to these basin-wide statistical patterns. We hope that continued analysis of these and related data sets, process models, and theoretical work will allow complex and compelling spicy seas, like the two discussed in this paper, to share their secrets with us. ©

REFERENCES

Batchelor, G.K. 1959. Small-scale variation of convected quantities like temperature in turbulent fluid. *Journal of Fluid Mechanics* 5:113–139, http://dx.doi.org/10.1017/S002211205900009X.

Belcher, S.E., A.L.M. Grant, K.E. Hanley, B. Fox-Kemper, L. Van Roekel, P.P. Sullivan, W.G. Large, A. Brown, A. Hines, D. Calvert, and others. 2012. A global perspective on Langmuir turbulence in the ocean surface boundary layer. *Geophysical Research Letters* 39, L18605, http://dx.doi.org/10.1029/2012GL052932.

Boccaletti, G., R. Ferrari, and B. Fox-Kemper. 2007. Mixed layer instabilities and restratification. *Journal of Physical Oceanography* 37:2,228–2,250, http://dx.doi.org/10.1175/JPO3101.1.

Callies, J., and R. Ferrari. 2013. Interpreting energy and tracer spectra of upper-ocean turbulence in the submesoscale range (1–200 km). *Journal of Physical Oceanography* 43 (11):2,456–2,474, http://dx.doi.org/10.1175/JPO-D-13-063.1.

Callies, J., G. Flierl, R. Ferrari, and B. Fox-Kemper. 2016. The role of mixed-layer instabilities in submesoscale turbulence. *Journal of Fluid Mechanics* 788:5–41, http://dx.doi.org/10.1017/jfm.2015.700.

Charney, J.G. 1971. Geostrophic turbulence. *Journal of the Atmospheric Sciences* 28(6):1,087–1,095, http://dx.doi.org/10.1175/1520-0469(1971)028<1087:GT>2.0.CO;2.

Chowdary, J.S., G. Srinivas, T.S. Fousiya, A. Parekh, C. Gnanaseelan, H. Seo, and J.A. MacKinnon. 2016. Representation of Bay of Bengal upper-ocean salinity in general circulation models. *Oceanography* 29(2):38–49, http://dx.doi.org/10.5670/oceanog.2016.37.

Cole, S.T., D.L. Rudnick, and J.A. Colosi. 2010. Seasonal evolution of upper-ocean horizontal structure and the remnant mixed layer. *Journal of Geophysical Research* 115, C04012, http://dx.doi.org/10.1029/2009JC005654.

Cottier, F., V. Tverberg, M. Inall, H. Svendsen, F. Nilsen, and C. Griffiths. 2005. Water mass modification in an Arctic fjord through cross-shelf exchange: The seasonal hydrography of Kongsfjorden, Svalbard. *Journal of Geophysical Research* 110, C12005, http://dx.doi.org/10.1029/2004JC002757.

Ferrari, R., and D. Rudnick. 2000. Thermohaline variability in the upper ocean. *Journal of Geophysical Research* 105(C7):16,857–16,883, http://dx.doi.org/10.1029/2000JC900057.

Fox-Kemper, B., G. Danabasoglu, R. Ferrari, S.M. Griffies, R.W. Hallberg, M.M. Holland, M.E. Maltrud, S. Peacock, and B.L. Samuels. 2011. Parameterization of mixed layer eddies: Part III. Implementation and impact in global ocean climate simulations. *Ocean Modelling* 39(1–2):61–78, http://dx.doi.org/10.1016/j.ocemod.2010.09.002.

Jinadasa, S.U.P., I. Lozovatsky, J. Planella-Morató, J.D. Nash, J.A. MacKinnon, A.J. Lucas, H.W. Wijesekera, and H.J.S. Fernando. 2016. Ocean turbulence and mixing around Sri Lanka and in adjacent waters of the northern Bay of Bengal. *Oceanography* 29(2):170–179, http://dx.doi.org/10.5670/oceanog.2016.49.

Johnston, T.M.S., D. Chaudhuri, M. Mathur, D.L. Rudnick, D. Sengupta, H.L. Simmons, A. Tandon, and R. Venkatesan. 2016. Decay mechanisms of near-inertial mixed layer oscillations in the Bay of Bengal. *Oceanography* 29(2):180–191, http://dx.doi.org/10.5670/oceanog.2016.50.

Klymak, J.M., W. Crawford, M.H. Alford, J.A. MacKinnon, and R. Pinkel. 2015. Along-isopycnal variability of spice in the North Pacific. *Journal of Geophysical Research* 120:2,287–2,307, http://dx.doi.org/10.1002/2013JC009421.

Kunze, E., J. Klymak, R.-C. Lien, R. Ferrari, C. Lee, M. Sundermeyer, and L. Goodman. 2015. Submesoscale water-mass spectra in the Sargasso Sea. *Journal of Physical Oceanography* 45(5):1,325–1,338, http://dx.doi.org/10.1175/JPO-D-14-0108.1.

Large, W., J. McWilliams, and S. Doney. 1994. Oceanic vertical mixing: A review and a model with a non-local boundary-layer paramaterization. *Reviews of Geophysics* 32(4):363–403, http://dx.doi.org/10.1029/94RG01872.

Lucas, A.J., E.L. Shroyer, H.W. Wijesekera, H.J.S. Fernando, E. D'Asaro, M. Ravichandran, S.U.P. Jinadasa, J.A. MacKinnon, J.D. Nash, R. Sharma, and others. 2014. Mixing to monsoons: Air-sea interactions in the Bay of Bengal. *Eos, Transactions American Geophysical Union* 95(30):269–270, http://dx.doi.org/10.1002/2014EO300001.

Lucas, A.J., J.D. Nash, R. Pinkel, J.A. MacKinnon, A. Tandon, A. Mahadevan, M.M. Omand, M. Freilich, D. Sengupta, M. Ravichandran, and A. Le Boyer. 2016. Adrift upon a salinity-stratified sea: A view of upper-ocean processes in the Bay of Bengal during the southwest monsoon. *Oceanography* 29(2):134–145, http://dx.doi.org/10.5670/oceanog.2016.46.

Mahadevan, A. 2016. The impact of sub-mesoscale physics on primary productivity of plankton. *Annual Review of Marine Science* 8:161–184, http://dx.doi.org/10.1146/annurev-marine-010814-015912.

Mahadevan, A., G. Spiro Jaeger, M. Freilich, M. Omand, E.L. Shroyer, and D. Sengupta. 2016. Freshwater in the Bay of Bengal: Its fate and role in air-sea heat exchange. *Oceanography* 29(2):72–81, http://dx.doi.org/10.5670/oceanog.2016.40.

Marcinko, C.L., A.P. Martin, and J.T. Allen. 2015. Characterizing horizontal variability and energy spectra in the Arctic Ocean halocline. *Journal of Geophysical Research* 120(1):436–450, http://dx.doi.org/10.1002/2014JC010381.

Prasad, T. 1997. Annual and seasonal mean buoyancy fluxes for the tropical Indian Ocean. *Current Science* 73:667–674.

Rocha, C.B., T.K. Chereskin, S.T. Gille, and D. Menemenlis. 2016. Mesoscale to submesoscale wavenumber spectra in Drake Passage. *Journal of Physical Oceanography* 46:601–620, http://dx.doi.org/10.1175/JPO-D-15-0087.1.

Rudnick, D.L., and J.P. Martin. 2002. On the horizontal density ratio in the upper ocean. *Dynamics of Atmospheres and Oceans* 36(1):3–21, http://dx.doi.org/10.1016/S0377-0265(02)00022-2.

Samelson, R. and C. Paulson. 1988. Towed thermistor chain observations of fronts in the subtropical North Pacific. *Journal of Geophysical Research* 93(C3):2,237–2,246, http://dx.doi.org/10.1029/JC093iC03p02237.

Sarkar, S., H.T. Pham, S. Ramachandran, J.D. Nash, A. Tandon, J. Buckley, A.A. Lotliker, and M.M. Omand. 2016. The interplay between submesoscale instabilities and turbulence in the surface layer of the Bay of Bengal. *Oceanography* 29(2):146–157, http://dx.doi.org/10.5670/oceanog.2016.47.

Schott, F.A., and J.P. McCreary Jr. 2001. The monsoon circulation of the Indian Ocean. *Progress in Oceanography* 51(1):1–123, http://dx.doi.org/10.1016/S0079-6611(01)00083-0.

Sengupta, D., G. Bharath Raj, M. Ravichandran, J. Sree Lekha, and F. Papa. 2016. Near-surface salinity and stratification in the North Bay of Bengal from moored observations. *Geophysical Research Letters* 43, http://dx.doi.org/10.1002/2016GL068339.

Shcherbina, A.Y., M.A. Sundermeyer, E. Kunze, E. D'Asaro, G. Badin, D. Birch, A.-M.E.G. Brunner-Suzuki, J. Callies, B.T. Guebel Cervantes, M. Claret, and others. 2015. The LatMix summer campaign: Submesoscale stirring in the upper ocean. *Bulletin of the American Meteorological Society* 96(8):1,257–1,279, http://dx.doi.org/10.1175/BAMS-D-14-00015.1.

Shroyer, E.L., D.L. Rudnick, J.T. Farrar, B. Lim, S.K. Venayagamoorthy, L.C. St. Laurent, A. Garanaik, and J.N. Moum. 2016. Modification of upper-ocean temperature structure by sub-surface mixing in the presence of strong salinity stratification. *Oceanography* 29(2):62–71, http://dx.doi.org/10.5670/oceanog.2016.39.

Smith, K.M., P.E. Hamlington, and B. Fox-Kemper. 2015. Effects of submesoscale turbulence on ocean tracers. *Journal of Geophysical Research* 121:908–933, http://dx.doi.org/10.1002/2015JC011089.

Smith, K.S., and R. Ferrari. 2009. The production and dissipation of compensated thermohaline variance by mesoscale stirring. *Journal of Physical Oceanography* 39(10):2,477–2,501, http://dx.doi.org/10.1175/2009JPO4103.1.

Subramanian, V. 1993. Sediment load of Indian rivers. *Current Science* 64:928–930.

Svendsen, H., A. Beszczynska-Møller, J.O. Hagan, B. Lefauconnier, V. Tverberg, S. Gerland, J.B. Ørbok, K. Bischof, C. Papucci, M. Zajaczkowski, and others. 2002. The physical environment of Kongsfjorden–Krossfjorden, an Arctic fjord system in Svalbard. *Polar Research* 21(1):133–166, http://dx.doi.org/10.1111/j.1751-8369.2002.tb00072.x.

Thangaprakash, V.P., M.S. Girishkumar, K. Suprit, N. Suresh Kumar, D. Chaudhuri, K. Dinesh, A. Kumar, S. Shivaprasad, M. Ravichandran, J.T. Farrar, and others. 2016. What controls seasonal evolution of sea surface temperature in the Bay of Bengal? Mixed layer heat budget analysis using moored buoy observations along 90°E. *Oceanography* 29(2):202–213, http://dx.doi.org/10.5670/oceanog.2016.52.

Thomas, L.N., A. Tandon, and A. Mahadevan. 2008. Submesoscale processes and dynamics. Pp. 17–38 in *Ocean Modeling in an Eddying Regime*. M.W. Hecht and H. Hasumi, eds, Geophysical Monograph Series, American Geophysical Union, Washington, DC, http://dx.doi.org/10.1029/177GM04.

Timmermans, M.-L. 2015. The impact of stored solar heat on Arctic sea ice growth. *Geophysical Research Letters* 42(15):6,399–6,406, http://dx.doi.org/10.1002/2015GL064541.

Timmermans, M.-L., S. Cole, and J. Toole. 2012. Horizontal density structure and restratification of the Arctic Ocean surface layer. *Journal of Physical Oceanography* 42(4):659–668, http://dx.doi.org/10.1175/JPO-D-11-0125.1.

Timmermans, M.-L., and S.R. Jayne. 2016. The Arctic Ocean spices up. *Journal of Physical Oceanography* 46(4):1,277–1,284, http://dx.doi.org/10.1175/JPO-D-16-0027.1.

Timmermans, M.-L., and P. Winsor. 2013. Scales of horizontal density structure in the Chukchi Sea surface layer. *Continental Shelf Research* 52:39–45, http://dx.doi.org/10.1016/j.csr.2012.10.015.

Varkey, M., V. Murty, and A. Suryanarayana. 1996. Physical oceanography of the Bay of Bengal and Andaman Sea. *Oceanography and Marine Biology: An Annual Review* 34:1–70.

Wang, D.-P., C.N. Flagg, K. Donohue, and H.T. Rossby. 2010. Wavenumber spectrum in the Gulf Stream from shipboard ADCP observations and comparison with altimetry measurements. *Journal of Physical Oceanography* 40(4):840–844, http://dx.doi.org/10.1175/2009JPO4330.1.

Warner, S.J., J. Becherer, K. Pujiana, E.L. Shroyer, M. Ravichandran, V.P. Thangaprakash, and J.N. Moum. 2016. Monsoon mixing cycles in the Bay of Bengal: A year-long subsurface mixing record. *Oceanography* 29(2):158–169, http://dx.doi.org/10.5670/oceanog.2016.48.

Wijesekera, H.W., E. Shroyer, A. Tandon, M. Ravichandran, D. Sengupta, P. Jinadas, H.J.S. Fernando, N. Agrawal, K. Arulanathan, G.S. Bhat, and others. In press. ASIRI: An Ocean-Atmosphere Initiative for Bay of Bengal. *Bulletin of the American Meteorological Society*, http://dx.doi.org/10.1175/BAMS-D-14-00197.1.

AUTHORS

Jennifer A. MacKinnon (jmackinnon@ucsd.edu) is Professor, Scripps Institution of Oceanography, University of California, San Diego, La Jolla, CA, USA. **Jonathan D. Nash** is Professor, College of Earth, Ocean, and Atmospheric Sciences, Oregon State University, Corvallis, OR, USA. **Matthew H. Alford** is Professor, Scripps Institution of Oceanography, University of California, San Diego, La Jolla, CA, USA. **Andrew J. Lucas** is Assistant Research Oceanographer, Scripps Institution of Oceanography, University of California, San Diego, La Jolla, CA, USA. **John B. Mickett** is Senior Oceanographer, Applied Physics Laboratory, University of Washington, Seattle, WA, USA. **Emily L. Shroyer** is Assistant Professor, College of Earth, Ocean, and Atmospheric Sciences, Oregon State University, Corvallis, OR, USA. **Amy F. Waterhouse** is Project Scientist, Scripps Institution of Oceanography, University of California, San Diego, La Jolla, CA, USA. **Amit Tandon** is Professor of Mechanical Engineering, University of Massachusetts Dartmouth, North Dartmouth, MA, USA. **Debasis Sengupta** is Associate Professor, Indian Institute of Science, Bangalore, India. **Amala Mahadevan** is Senior Scientist, Woods Hole Oceanographic Institution, Woods Hole, MA, USA. **M. Ravichandran** is Head, Observations and Modeling, Indian National Centre for Ocean Information Services, Hyderabad, India. **Robert Pinkel** is Professor Emeritus, Scripps Institution of Oceanography, University of California, San Diego, La Jolla, CA, USA. **Daniel L. Rudnick** is Professor, Scripps Institution of Oceanography, University of California, San Diego, La Jolla, CA, USA. **Caitlin B. Whalen** is Research Associate, Applied Physics Laboratory, University of Washington, Seattle, WA, USA. **Marion S. Alberty** is a graduate student at Scripps Institution of Oceanography, University of California, San Diego, La Jolla, CA, USA. **J. Sree Lekha** is a graduate student at the Centre for Atmospheric and Oceanic Sciences, Indian Institute of Science, Bangalore, India. **Elizabeth C. Fine** is a graduate student at Scripps Institution of Oceanography, University of California, San Diego, La Jolla, CA, USA. **Dipanjan Chaudhuri** is a graduate student at the Centre for Atmospheric and Oceanic Sciences, Indian Institute of Science, Bangalore, India. **Gregory L. Wagner** is a recent PhD recipient at Scripps Institution of Oceanography, University of California, San Diego, La Jolla, CA, USA.